Miscible Blend Dynamics and Thermodynamics: Quantitatively Untangling Slow Conformational Events in Amorphous Polymer Mixtures

Marcin Wachowicz and Jeffery L. White*

Department of Chemistry, Oklahoma State University, Stillwater, Oklahoma 74078

Received March 12, 2007; Revised Manuscript Received May 14, 2007

ABSTRACT: Chain dynamics in macromolecules that occur with slow characteristic exchange frequencies (1−100 Hz) influence the bulk mechanical properties of polymers. In this contribution, we systematically evaluate the change in conformational reorientations of individual polymer backbones once they form a miscible binary blend, using the solid-state CODEX NMR experiment over a 100 K temperature range. The temperature range encompasses the glass-transition points of each pure polymer. The high molecular weight polyisobutylene (PIB)/head-to-head polypropylene (hhPP) polymer blend is known to form an intimate mixture at the 50:50 wt % composition used in this study. Detailed site-specific measurements and analysis of slow polymer backbone dynamics in the pure and blend state reveal that the two blended components converge to a common averaged temperature where slow chain motion is maximized in each chain type with equal correlation times, but unique exchange intensity distributions and activation barriers are preserved for each polymer. Most interestingly, the value of this composition-weighted average temperature is 5−7 deg lower than predicted using the Fox equation, quantitatively confirming our previous assignments of configurational entropy as a miscibility driver in polyolefin blends. Quantitative estimates of the log-Gaussian correlation time distribution models and their temperature dependence are discussed with respect to the activation energies E_a for slow backbone reorientation in pure amorphous PIB, pure amorphous hhPP, and each in the miscible blend; emphasis is directed toward changes in the models induced by formation of the miscible blend relative to the pure components. By direct comparison of data obtained using identical experimental parameters, chain dynamics are relatively more perturbed for hhPP, the high-T_g blend component, than for PIB (−30 K vs +15 K, respectively, for the temperature of maximum slow exchange density relative to the pure material), in agreement with previously published conclusions. Using an Adams−Gibbs model as the most reasonable physical model suggested by the data, we calculate an increase in the configurational entropy S_c of the miscible blend relative to the unmixed components ranging from 11 to 17%. Importantly, all data are specifically extracted from individual signals arising from each polymer in the solid blend, rather than bulk-averaged responses, and without any form of sample modification.

Introduction

Defining structure and dynamics in complex systems of amorphous macromolecules is a common goal for modern research in materials science. Many questions are as equally relevant to understanding end-use properties in polymer blends and composites as they are for predicting the organization of proteins in a tertiary structure.[1−3] How do macromolecules of varying polarity and functional group density organize themselves at the local chain level? How does this organization change with the introduction of a mixed system? Recently, several groups including our own have investigated these questions using polyolefin blends as a limiting class of macromolecules in which specific chemical interactions are minimized due to their completely saturated sp^3 carbon structure.[4−14] In addition to the inherent fundamental understanding to macromolecular thermodynamics afforded by the unique chemical structure of polyolefin blends, mixtures of polyolefins comprise one of the most economically important polymer systems. Chain organization and dynamics control the observed mechanical properties, and while many polyolefin blends are semicrystalline, important limits on phase behavior can be established by examination of amorphous blends. To this end, we have reported experiments that identify configurational entropy as a key thermodynamic parameter in miscible polyolefin blends,[10,11,13] which is supported by recent theoretical papers.[15−17] Several groups have demonstrated that blends of polyisobutylene (PIB) and head-to-head polypropylene (hhPP) form one such miscible system.[4,8,14] In this contribution, direct chain-level CODEX NMR experiments on slow backbone conformational dynamics in the PIB/hhPP blend allow simultaneous, yet specific, examination of each polymer component over a wide temperature range. The CODEX solid-state NMR experiment, recently developed by Schmidt-Rohr and coworkers,[18] is a versatile and powerful experimental probe of slow chain motions in macromolecules.[19−21] Quantitative analysis of dynamic events (for each polymer chain) in the mechanically relevant 1−100 Hz time scale, using CODEX NMR data and detailed physical models of chain motion, reveal that chain dynamics in the high-T_g hhPP component are relatively more perturbed than PIB upon miscible blend formation. While slow backbone conformational exchange intensity converges to a common temperature for both the PIB and hhPP component in the blend, this common temperature is below that predicted by the Fox equation. The quantitative data and supporting conclusions from all data analyses, including characteristic exchange time constants for the slow motions, confirm that increased configurational entropy is an important thermodynamic parameter for polyolefin miscibility. Moreover, we demonstrate that differential dynamics in miscible polymer mixtures for specific polymer chains is quantitatively accessible using the CODEX experimental approach, a powerful alternative compared to

* To whom all correspondence should be addressed. E-mail: jeff.white@okstate.edu.

10.1021/ma070605g CCC: $37.00
Published on Web 06/20/2007

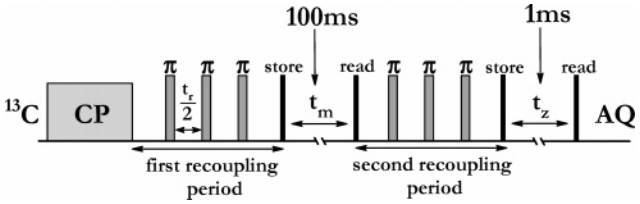

Figure 1. CODEX experiment pulse sequence, showing only the pulses for the carbon channel. Radio-frequency pulses for the proton channel have been omitted for clarity. The value of the exchange mixing time $t_m = 100$ ms for all PIB, hhPP, and blend data reported in this paper. The total time corresponding to the sum of the first and second recoupling period $2(2t_r) = 1$ ms.

previous studies on miscible blend dynamics[22−25] and one which until this time has been limited to studies of single polymer systems.

Experimental Section

Samples and Data Collection. Polyisobutylene ($M_w = 1\,000\,000$) was purchased from ExxonMobil Chemical, and hhPP was prepared by hydrogenation of poly(2,3-dimethylbutadiene) obtaining a $M_w = 50\,000$. The 50:50 wt % PIB/hhPP (43:57 mol %) blend was prepared by dissolution in toluene over 2 days followed by evaporation and vacuum drying for 4 days. DSC measurements indicated glass transitions for PIB and hhPP of −68 and −20 °C, respectively. All ^{13}C and ^{1}H measurements were collected on a Bruker DSX-300 with field strength = 7.05 T. Solid-state CODEX NMR experiments were performed on a 4 mm double-resonance magic-angle spinning probe using the previously described sequence from Schmidt-Rohr.[18] The probe temperature was calibrated using $PbNO_3$ to within ±1 K. All CODEX exchange data were acquired with an actively controlled 4 kHz MAS speed, a 1 ms cross-polarization contact time, and rotor synchronization, and as a precaution, CODEX measurements were altered between the CODEX and reference signal every 256 scans to eliminate spectrometer drift. All CODEX slow exchange data were acquired using a 100 ms exchange time, unless otherwise noted. Total experiment times typically ranged between 8 and 12 h for a single measurement. For reference, the pulse sequence is shown in Figure 1 along with the exact values used for mixing and recoupling times.

Calculations and Theory. Chain conformational exchange data from the CODEX experiments were analyzed to extract correlation time constants, activation energies for chain reorientation, and quantitative correlation time distributions. An isotropic rotational diffusion model (employing 20 discrete conformer populations as an approximation to the heterogeneous backbone conformer distribution) was used to simulate the experimental data and solve the overall equilibrium exchange matrix as a function of the exchange mixing time in the CODEX experiment and the correlation time constant for the specific polymer at each temperature.[21,26−28] A discrete log-Gaussian correlation time distribution function was analyzed with respect to temperature using both Arrhenius and WLF models. Powder averaged values of the chemical shift anisotropy, reflecting the distribution of tensor orientations in the amorphous polymers, were included in all calculated fits of the data. The *Mathematica* program (version 5.2) was used for all calculations. The theory regarding exchange intensities has been previously developed for static samples, and the incorporation of the additional terms arising from the time dependence of the frequency introduced by MAS has also been described.[28] With the current detailed and extensive application to a polyolefin blend system of interest, we have demonstrated an appealing capability for the CODEX experiment in polymer blend science. Complete details for all calculations are included in the Supporting Information. For convenience, the equation describing the quantitative evolution of the normalized exchange intensity **E** as a function of exchange time and temperature for a distribution of correlation times $g(\tau)$ is reproduced here:[21]

$$E(t_m,\tau_c,T) = \frac{S_0 - S}{S_0} = \frac{\int_0^\infty \{\mathrm{Re}[G_-(t_z,\tau,T)] - \mathrm{Re}[G_-(t_m,\tau,T)]\} g(\tau)\, d\tau}{\int_0^\infty \mathrm{Re}[G_-(t_z,\tau,T)] g(\tau)\, d\tau}$$

All additional terms are defined and described in the Supporting Information, but the reader can quickly note the time dependencies for the specific delays in the Figure 1 pulse sequence.

Results and Discussion

Control Experiments and Experimental Strategy. Although several groups, including our own, have recently used the CODEX approach to investigate polymers, the following example is informative for those not familiar with the experimental details. Simply stated, the experiment is a one-dimensional constant-time version of classic two-dimensional exchange experiments that exploits the anisotropy of the chemical shift interaction to detect movement (in real time) of polymer chain segments. Figure 2 shows the discrete steps in obtaining CODEX exchange data for a semicrystalline polypropylene sample. This PP sample (Polysciences) was nominally atactic, but solution NMR revealed significant isotacticity present, in agreement with DSC results. We observe that the pure CODEX result **(**Δ*S***)** at 260 K (bottom spectrum in Figure 2) generates a spectrum containing peaks arising predominantly from the conformationally heterogeneous amorphous PP chains. In other words, the pure CODEX spectrum will only contain signal intensity for chain segments that have reoriented during the allowed exchange/mixing time, resulting in a different chemical shift anisotropy magnitude which is not refocused during the second recoupling period, consequently generating a signal in the pure CODEX difference spectrum. Conversely, control experiments on a crystalline organic solid, methylmalonic acid, yield zero intensity in the pure CODEX spectrum, as expected for a rigid crystalline material (not shown).[18] As we have previously published, detailed control experiments on crystalline bisphenol A, in which CODEX and 2D NMR exchange data are compared, indicate that the CODEX data are quantitative and free from any artifacts that may affect signal intensity in the pure exchange analysis.[13,29]

Similarly, CODEX data for a fixed 100 ms mixing time were collected for pure PIB, pure hhPP, and their 50:50 wt % blend at temperatures ranging from 205 to 308 K. On average, 15 different temperature points were run for each of the three samples, and since a reference and exchange spectrum must be measured at each temperature, ∼100 individual CODEX measurements were completed. Three representative spectra, taken at different temperatures, are shown in Figure 3 for each of the pure polymers and the blend.

Only the signals that were used in deconvoluted area calculations are labeled in each spectrum; the signals correspond to the methyl carbons from hhPP (10−25 ppm region) and the quaternary backbone carbon from PIB (39 ppm). These particular signals were selected due to their relatively high resolution and the fact that their individual dynamic behavior directly tracks that of the polymer backbone. Figure 4 quantitatively demonstrates the latter point, using several different mixing times (at the same temperatures as used for the spectra in Figure 3) to determine the exchange correlation time constant. For example, Figure 4a shows the growth of the CODEX exchange signal vs exchange mixing time for pure hhPP. Irrespective of whether the side-chain methyl or backbone methylene/methine carbons are used to follow the exchange, a

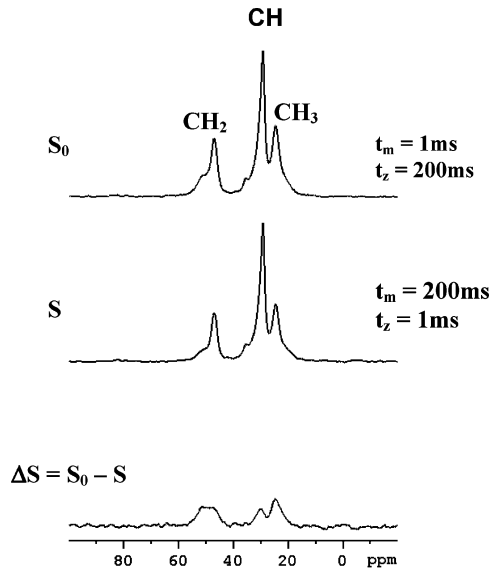

Figure 2. Pure-CODEX spectrum (ΔS) is obtained via subtraction of the CODEX (S) from the reference (S_0), as illustrated for PP. The spectra were obtained with spinning speed of 4 kHz, $Nt_r = 500$ μs, mixing time = 200 ms, scans = 12K, and line broadening = 75 Hz.

common correlation time constant of 18.9 ± 2.3 ms is obtained using a single correlation time function at 276 K. Therefore, we can use the hhPP CH_3 signal as an accurate reporter of backbone chain dynamics. Figure 4b shows similar CODEX exchange data for pure PIB at 227 K. In order to quantitatively address the difference in exchange intensity with CSA recoupling time, the PIB quaternary signal (C_q) was measured for two different recoupling times equal to 1 and 2 ms. Using slow spinning experiments at 227 K, the temperature for the data shown in Figure 4b, we determine that $\delta\tau_{csa} \geq 5$ and 10 at 1 and 2 ms recoupling, respectively. While the absolute exchange intensity does increase for PIB at the longer recoupling time, Figure 4b shows that the same exchange correlation time constant is obtained in each case (26 ± 3 ms vs 30 ± 7 ms), within the error of the experiment. Indeed, while the absolute exchange intensity does increase at 2 ms recoupling, the actual signal-to-noise of the measurement goes down due to increased spin−spin relaxation during the longer recoupling time, resulting in a slightly larger uncertainty relative to the 1 ms data. As Schmidt-Rohr and co-workers have discussed at length in ref 21, there are several factors that must be considered in determining the absolute maximum value of an $E(T)$ point. One competing mechanism is molecular motion interference with coherent proton decoupling over a temperature range. For PIB, we know from previous work that the quaternary carbon is most immune to this complicating factor over this temperature range. Additional complications regarding motions in intermediate or very high-frequency regions can affect individual $E(T)$ values, again as discussed in detail in ref 21. However, quantitative comparisons of relative temperature-dependent behavior for pure polymers vs the same polymers in a blend are accessible using a fixed set of experimental conditions, as we will show in the remaining sections.

These two example temperatures were specifically chosen due to their proximity to the exchange intensity maximum for each pure sample (vide infra). Therefore, it is not surprising that similar correlation time constants (19 vs 26 ms) for backbone motion are obtained for each polymer. As explained in detail in the Supporting Information and in ref 20, the correlation time constant window selected in the CODEX experiment is 1−100 ms, and one should expect that the maximum exchange intensity signal is obtained for intermediate correlation time constants for both polymers.

The final type of experimental data required to establish baseline behavior for a pure, unmixed polymer is the temperature-dependent normalized exchange intensity for backbone conformational dynamics. As an example, Figure 5a shows the normalized CODEX exchange intensity vs temperature for pure hhPP over an 80 K range and including the DSC T_g temperature. Indeed, the onset of detectable exchange intensities $E(T)$ corresponds almost exactly with the DSC T_g of 253 K, demonstrating that the CODEX experiment probes a time scale familiar to many polymer scientists.

In Figure 5a, the solid lines through the data points are fits to the experimental CODEX data using a full powder-averaged simulation for a sample undergoing 4 kHz MAS. As previously mentioned and explained in detail in the Supporting Information, fits to all CODEX data in this paper are obtained via a 20-site rotational isotropic diffusion model for solving the exchange matrix, with a discrete log-Gaussian correlation time distribution for backbone motion. Intuitively, the dispersion in segmental conformational exchange correlation time constants will decrease as the temperature increases in an amorphous macromolecule,[30] becoming most homogeneous in the liquidlike regime far above T_g. Figure 5b shows the calculated temperature-dependent widths of the log-Gaussian correlation time distributions $\sigma(T)$ for pure hhPP to exemplify the techniques described in the Supporting Information. In this model, the width of the correlation time distribution $\sigma(T)$ varies linearly with temperature, as shown by the line in Figure 5b. To clarify, Figure 6 demonstrates graphically how the distribution of exchange correlation time constants varies at six selected temperatures for blended (a−c) and pure (d−f) hhPP in our discrete (17 points) log-Gaussian model. We assume an Arrhenius model for the temperature dependence of the mean correlation time τ_c.

The quantitative relationships between $\sigma(T)$ and the weighting factors $g(\tau)$ for each correlation time used in the exchange intensity simulations are discussed in the Supporting Information. On the basis of the data and methods reflected in Figures 5 and 6, we can now specifically and quantitatively interrogate the individual slow polymer chain motions, through the normalized exchange intensities $E(T)$ and the correlation time distributions, upon formation of the miscible hhPP/PIB blend and compare them to the results for each pure polymer component.

Pure Polymer vs Polymer Blend Exchange Intensities. Figure 7 summarizes the total CODEX slow conformational exchange data for pure PIB, pure hhPP, and the miscible blend.

Smooth lines through the data points in Figure 7 were calculated as described above, resulting in the temperature-dependent correlation time distribution widths $\sigma(T)$ shown in Figure 8. The three specific temperature points shown on each line in Figure 8 were chosen to illustrate low- and high-temperature limits for CODEX signal detection and also near the exchange intensity maximum. The values of $\sigma(T)$ we extract from the $E(T)$ fits are consistent with previous reports, albeit for different polymer systems.[20,27] For each polymer, we find an increased temperature dependence upon blend formation, intuitively consistent with the formation of a more heterogeneous amorphous morphology. This result, along with the identical $E(T)$ maximum temperature in Figure 7, indicates that the blend is intimately mixed at the chain level.

Although an identical $E(T)$ maximum temperature for the polymer components in the blend is observed in Figure 7, the relative behavior of the two polymers is unique. First, the shift in the $E(T)$ maximum temperature of the hhPP upon blend

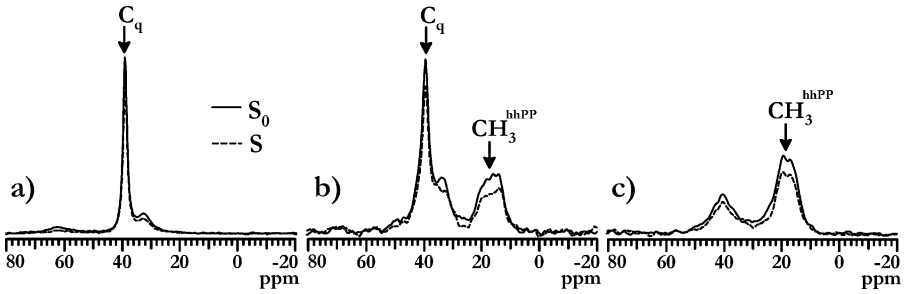

Figure 3. Example CODEX spectra for (a**)** pure PIB at 230 K, (b**)** PIB/hhPP blend at 250 K, and (c**)** pure hhPP at 273 K, all obtained with a 100 ms exchange time.

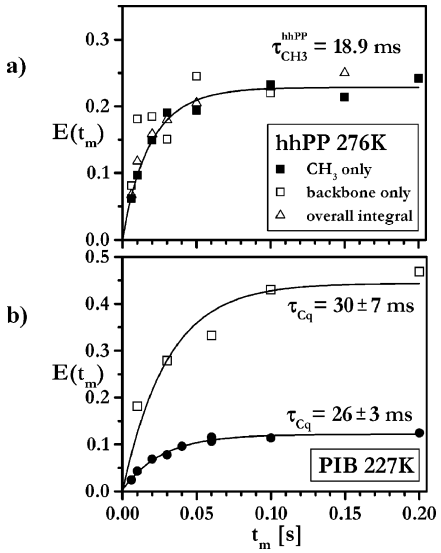

Figure 4. Normalized exchange intensities $E(t_m)$ plotted vs mixing time for (a) pure hhPP, exhibiting an exchange correlation time constant = 18.9 ± 2.3 ms, and (b) pure PIB, obtained using a total CSA recoupling time for C_q of 1 ms (bottom curve) and 2 ms (top curve). Note that within experimental error the same exchange correlation time constant is obtained in (b) for the two different recoupling times. These example temperatures (indicated) were chosen since they are near the temperature corresponding to the maximum exchange intensity for each pure sample. As described in the text, the hhPP CH_3 signal and the PIB C_q signal are used to follow chain conformational dynamics in the pure materials and their respective chains in the blend.

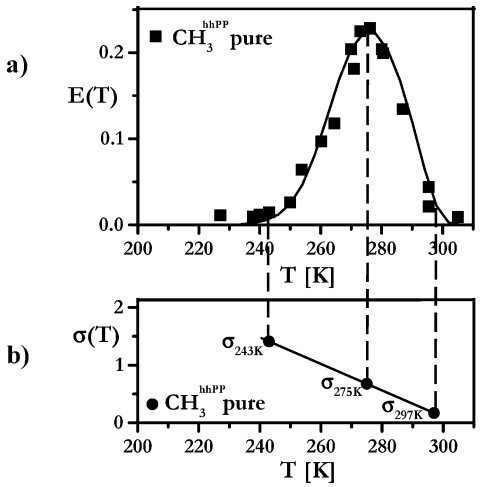

Figure 5. (a**)** Normalized exchange intensities $E(T)$ vs temperature for pure bulk hhPP. (b**)** Temperature dependence of the correlation time distribution widths $\sigma(T)$.

formation is −30 K, while that for PIB is only +15 K; this disparity is significantly greater than that expected for linear mixing rules in a 50:50 wt % blend. Second, while the width (ΔT) of the exchange intensity curves in Figure 7 increases slightly upon blend formation for both PIB and hhPP relative to each pure state, the curves maintain their absolute exchange intensity maximum value and overall relative shape. In other words, the conformational exchange intensity values are not averaged in the blend, even though the blend constituents are intimately mixed and the exchange intensity maxima are observed at the same temperature (246−247 K). Compared to the broad, featureless glass transition observed in a standard DSC experiment for the PIB/hhPP blend (not shown; $T_g \approx 230$ K), the $E(t_m)$ curves of Figure 7 provide detailed, chain-specific information about slow dynamics for each polymer in the blend. Note that the onset of exchange intensity for each pure polymer in Figure 7 exactly corresponds to the DSC T_g values reported in the Experimental Section. As shown in Figure 7, the observed exchange intensity maximum is 5−7 deg lower than predicted by the Fox equation for this blend composition (vide infra).

Activation Energies and Correlation Time Distributions. Figure 9 summarizes the results of the calculated fits to the experimental CODEX data of Figure 7 for the pure polymers and the polymers in the miscible blend. Within the error limits of the CODEX data from which the fitting parameters were extracted, E_a values are unchanged for each polymer upon blend formation. In agreement with the raw data in Figure 7, Figure 9a shows that the large decreases in chain correlation time constant for hhPP in the blend (∼3 decades at any T) are not offset by comparable increases in τ_c for PIB in the blend (∼1 decade at any T, Figure 9b). The vertical bars in Figure 9a,b indicate the width of the correlation time distribution at each temperature point. The PIB activation energy value is higher than the 60 kJ/mol value recently reported by deAzevedo et al.[21] However, we note that the data used to extract this lower value was for a static version of the exchange experiment (PUREX), which only provided one-half of the total normalized exchange intensity curve due to sensitivity limitations, and that the WLF function was used to extract the Arrhenius activation energy with reasonable values of the preexponential factor. We recognize that extrapolation of the Arrhenius fits in Figure 9 to infinite temperature will not give reasonable preexponential values τ_0 and that the E_a values in Figure 9 are most likely slightly higher than the actual value for each amorphous polymer (although they are well within ranges reported for amorphous and semicrystalline polymers). Our primary objective is to demonstrate the change in slow chain motions that occurs upon formation of the miscible blend, and we feel that the consistent application of a log-Gaussian correlation time distribution model (thereby requiring an Arrhenius temperature analysis) is the most physically intuitive and accurate approach. To be complete, however, a WLF/KWW analysis of the raw CODEX data for the pure hhPP is shown in Figure 10. The WLF fitting parameters are given in the caption for Figure 10a and result in

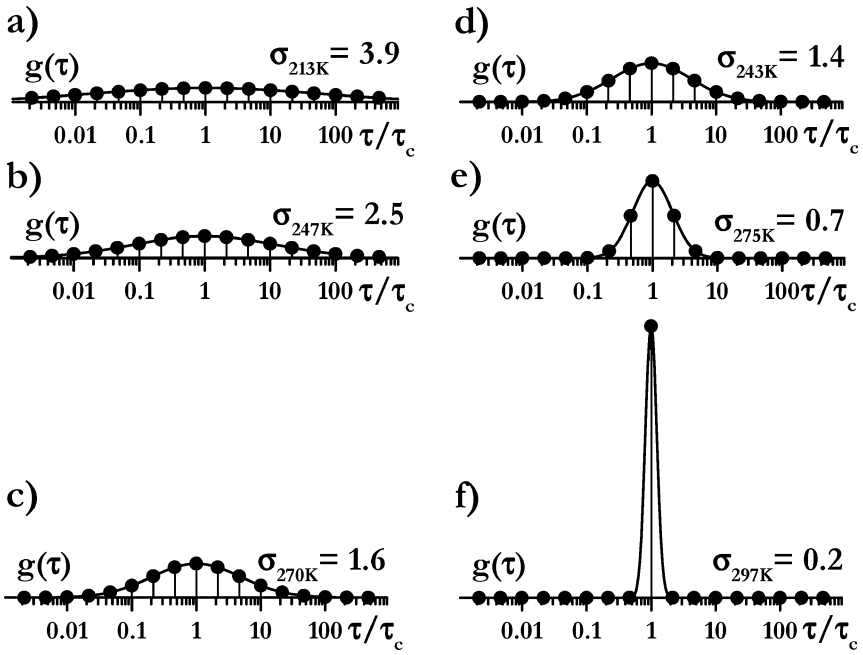

Figure 6. Discrete version of log-Gaussian distribution characterized by different widths σ at six specific temperatures for hhPP. The 17 points are centered at τ_c, and are equally spaced over 6 decades. The solid line is the continuous function. The value of σ is given at the right of each trace. (a) hhPP in blend at 213 K, (b) hhPP in blend at 247 K, (c) hhPP in blend at 270 K, (d) pure hhPP at 243 K, (e) pure hhPP at 275 K, and (f) pure hhPP at 297 K.

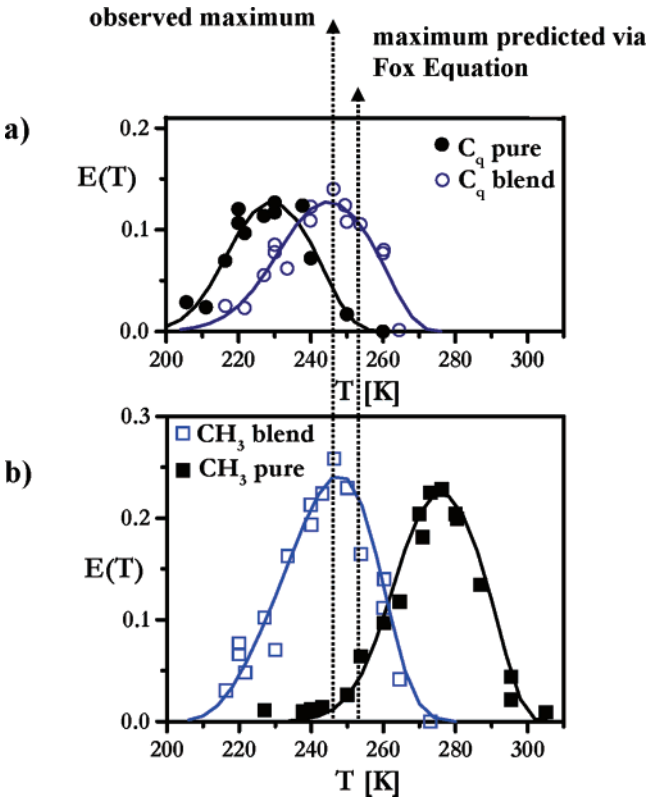

Figure 7. Normalized exchange intensities $E(t_m)$ for (a) pure PIB (●) and PIB in the blend (○) and (b) pure hhPP (■) and hhPP in the blend (□). Note the common exchange maximum temperature $T = 246$ K for each polymer in the blend (left arrow) and the Fox equation prediction (right arrow). The smooth lines are fits to the data as described in the text.

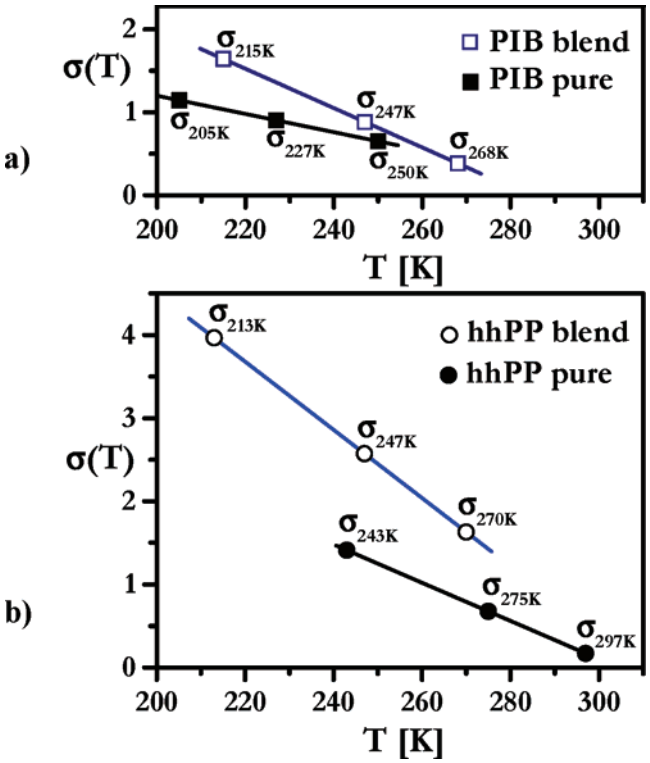

Figure 8. Correlation time distribution widths $\sigma(T)$ for (a) pure PIB and PIB in blend and (b) pure hhPP and hhPP in blend.

correlation time values that coincide with those obtained from the correlation time distribution/Arrhenius model over the temperature range of our experimental data (Figures 7−9). An Arrhenius function with $E_a = 124$ kJ/mol is justified as an approximation to the WLF function in the temperature range used here. As expected, at higher temperatures the Arrhenius function diverges from the WLF function, leading to unrealistic values of τ_0.

Validity of Model Extracted from Intermediate $\delta\tau_{csa}$ Experimental Parameters. In generating the data for PIB used in the fits for Figure 7, the shorter recoupling time = 1 ms from Figure 4b was used. To be complete, we must consider any effect this might have on our interpretations, both in terms of the temperature at which any $E(T)_{max}$ is observed and in terms

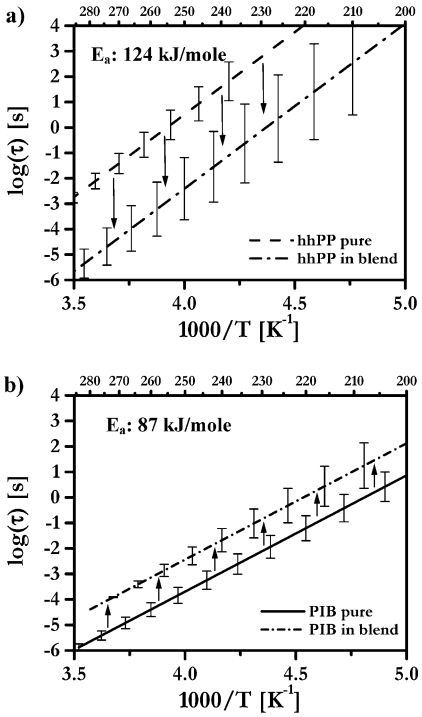

Figure 9. Temperature dependence of correlation time constants and resulting Arrhenius activation energies for (a**)** hhPP and (b**)** PIB. The vertical bars indicate the width of the log-Gaussian correlation time distribution at each temperature point, centered about τ_c. For clarity, only every second temperature point used in the calculation is shown.

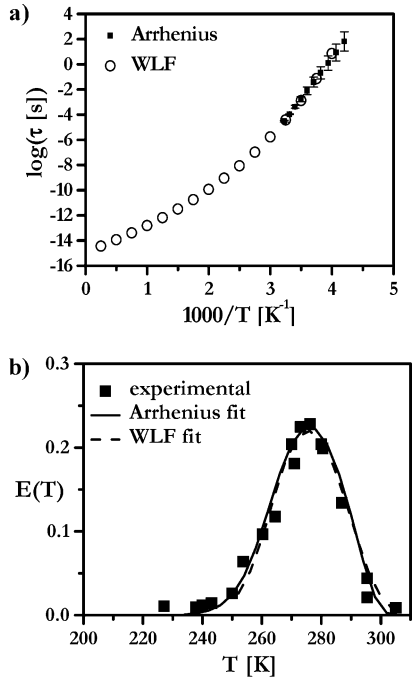

Figure 10. (a**)** Comparison of temperature-dependent correlation time constants for pure hhPP using WLF/KWW vs Arrhenius models discussed in text. The WLF parameters for this pure hhPP fit are $C_1 = 15.5$, $C_2 = 117$, $\tau(T_g) = 4.52$ s, and $T_g = 252$ K. (b**)** Comparative fits to the experimental CODEX exchange intensity data for 12-point discrete KWW/WLF model (dash) vs correlation time distribution Arrhenius model (solid); $\beta = 0.66$ in the KWW model.

of the correlation times and distributions extracted from the data. We note several things about the temperature-dependent $E(T)$ curves for the pure polymers and the blend in Figure 7 that indicate that the recoupling time cannot influence the temperature of the maximum observed $E(T)$, even if it does control

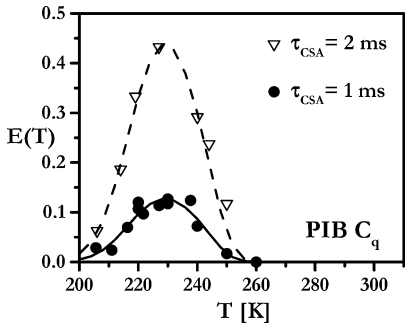

Figure 11. Temperature-dependent $E(T)$ curves for PIB obtained with (●) 1 ms and (▽) 2 ms CSA recoupling times. Quantitative fits extracted from the 1 ms data (solid line) were used to predict the 2 ms data fit (dashed line) prior to actually obtaining the 2 ms data points.

the absolute intensity of any specific point in the temperature distribution. The onset of detectable exchange intensity in each $E(T)$ curve shown in Figure 7 almost exactly mirrors their respective DSC T_g's. For PIB, the DSC value is 205 K; this is exactly where we begin to detect a measurable exchange component in Figure 7. For hhPP, the DSC value is ca. 250 K, and intensity begins above background at 245−250 K for that pure component in Figure 7. The relationship between the onset of intensity in the $E(T)$ curve, which is shown to be reliable by comparison to DSC, and the curve maximum is just temperature. Further, it demonstrates that we are not probing an anomalous response from some dilute component that is not representative of the bulk behavior. We also note that the both the temperature at which we detect the onset of exchange intensity for PIB in Figure 7, and the temperature for the exchange intensity maximum for PIB in Figure 7, agree almost exactly with the static PUREX values for PIB in Figure 11 of ref 21, even though there are large differences in the absolute value of $E(T)$ in the PUREX vs our CODEX results.

An experimental proof of this conclusion for our system is shown in Figure 11, where the temperature-dependent response of the CODEX $E(T)$ values are plotted for PIB for both 1 and 2 ms CSA recoupling times. Using the same correlation time distribution model described in the preceding sections, and which was extracted from the 1 ms recoupling time data, we accurately predicted the values of $E(T)$ for a new 2 ms recoupling time prior to actually obtaining the experimental data. Both sets of data, and their respective fits, are shown in Figure 11. This result confirms that the CODEX approach is extremely versatile for polymer blend studies, in that although the absolute maximum $E(T)$ intensity may not be accessible at each temperature due to competing mechanisms which degrade signal intensity,[21] quantitative fits with predictive power for comparisons of pure and blended polymers can be extracted from the raw data. Correlation time values τ_{ex} at the center of the distribution, extracted from either curve in Figure 11, are identical.

Negative Deviation from Fox Equation, Configurational Entropy, and Polyolefin Miscibility. Examination of the exchange maximum temperature from Figure 7 reveals a common value (246−247 K) for both PIB and hhPP chains in the miscible blend. The most widely used additivity rule for glass-transition temperatures in two-component, one-phase polymer blends is the Fox equation.[31] A reduced form of the Gordon−Taylor formalism, the Fox equation, produces a lower value of T_g than a simple linear mixing rule would predict due to the increased free volume expected to exist in a mixture of dissimilar polymer structures. Applying the Fox equation to our slow exchange CODEX data from Figure 7, i.e.

$$[(T_{em})^{-1}]_{blend} = w_{pib}/(T_{em})_{pib} + w_{hhpp}/(T_{em})_{hhpp}$$

where T_{em} equals the observed CODEX exchange maximum temperature for each component in Figure 7 (232 and 276 K), reveals that the *expected* exchange maximum temperature for the 50:50 wt % miscible PIB/hhPP blend is $[(T_{em})]_{blend} = 252$ K. A simple additive Gordon−Taylor expression would yield $[(T_{em})]_{blend} = 254$ K. The direct observation of backbone chain dynamics indicates an excess entropy contribution in this miscible polyolefin blend, in agreement with our previous experiments.

Recent interest in the spatial heterogeneity of the glass transition in amorphous macromolecules is inextricably linked to entropic arguments.[32−37] From our experimental perspective involving direct and selective polymer chain inspection using solid-state NMR methods, all data are in agreement with an Adams−Gibbs model for entropy and dynamic heterogeneity.[38] The heterogeneous distribution of cooperatively rearranging regions near the glass transition, as reflected in the correlation time distribution model used to accurately fit the low-temperature region of each experimental curve in Figure 7, becomes increasingly smaller (in absolute size) as the temperature is increased. Correspondingly, the correlation time distribution itself narrows with increasing temperature. While such arguments are usually discussed relative to single-component glass formers in the solid and liquid states (glass vs melt), they are equally applicable to the pure vs blended polymers. Simply stated, the entropy density increases with increasing temperature and decreasing volume of the cooperatively rearranging region. The fact that PIB and hhPP can form a stable miscible mixture in the absence of specific molecular interactions is consistent with larger entropy density increases relative to either of the pure, unmixed materials per energy unit *kT*. The significant deviation from the Fox equation prediction clearly indicates that the entropic penalty paid by the PIB component in forming the miscible blend with hhPP is more than compensated by the entropy gain for the hhPP chains in the miscible blend. Quantitatively, the change can be evaluated using the Adams−Gibbs equation

$$\tau_{ex} = \tau_0 \exp(c/TS_c)$$

where we equate τ_{ex} to τ_c, the value of the correlation time at the center of the distribution at $(T_{em})_{blend}$. Using Figures 7 and 9, and assuming τ_0 ranging from 10^{-12} to 10^{-15} s and c as constant for each polymer in pure vs mixed state at that fixed temperature $(T_{em})_{blend} = 246$ K, we determine that the change in configurational entropy for PIB chains ranges from −0.87 to −0.91 upon blend formation, while the corresponding scaling factor range for hhPP is +1.29 to +1.22, respectively. In total for both PIB and hhPP, $(S_c)_{blend}$ ranges from $1.16(S_c)_{unmixed}$ to $1.12(S_c)_{unmixed}$, meaning that there is an 11−16% increase in the total configurational entropy of the miscible blend compared to the two unmixed components. Therefore, one must conclude that an increase in the number of surface contacts either between dissimilar polymer chains or within chains themselves (an enthalpic model) in this miscible polyolefin blend simply does not exist relative to the unmixed pure polymers. This entropy ratio increase is very conservative, as its absolute value depends on the choice of τ_0. Again, the 1 order of magnitude increase in τ_c for PIB at $(T_{em})_{blend}$ cannot compensate for the 3 orders of magnitude decrease in hhPP's τ_c at $(T_{em})_{blend}$, as shown in Figure 9. The ability to noninvasively, selectively, and quantitatively determine such characteristic data for amorphous polymers in a miscible mixture is a key advantage of this experimental approach.

Conclusions

Direct, selective, and noninvasive inspection of chain dynamics in polymers comprising a binary miscible blend is quantitatively accessible using the solid-state CODEX NMR experiment. Using a rotational isotropic diffusion model coupled with a temperature-dependent correlation time distribution, slow conformational dynamics in pure PIB and pure hhPP change upon formation of their miscible blend in a manner consistent with a positive configurational entropy of mixing. Detailed site-specific measurements and quantitative analysis of slow polymer backbone dynamics in the pure and blend state of each polymer reveal that the two blended components converge to a common averaged temperature where slow chain motion is maximized in each chain type and with equal average correlation times, but unique exchange intensity distributions and activation barriers are preserved for each polymer. An Adams−Gibbs model satisfactorily explains the low-temperature deviation in the slow exchange dynamics relative to that predicted by Fox/Gordon−Taylor equations of mixing. We conclude that miscibility in at least some polyolefin blends must be driven by a positive configurational entropy of mixing, which for the PIB/hhPP blend examined here amounts to a 11−16% increase relative to the pure unmixed polymers.

Acknowledgment. The authors thank the National Science Foundation for support of this work through Grants DMR-0137968 and 0611474. Support for research instrumentation was provided by North Carolina State University and Oklahoma State University.

Supporting Information Available: Details of calculation of normalized exchange intensity and distribution of correlation times. This material is available free of charge via the Internet at http://pubs.acs.org.

References and Notes

(1) Lohse, D. J.; Graessley, W. W. In *Polymer Blends: Formulation and Performance*; Paul, D. R., Bucknall, C. B., Eds.; Wiley: New York, 2000; Vol. 1, p 219.
(2) Olsson, M. H. M.; Parson, W. W.; Warshel, A. *Chem. Rev.* **2006**, *106*, 1737.
(3) Stone, M. J. *Acc. Chem. Res.* **2001**, *34*, 379.
(4) Krishnamoorti, R.; Graessley, W. W.; Fetters, L. J.; Garner, R. T.; Lohse, D. J. *Macromolecules* **1995**, *28*, 1252.
(5) Graessley, W. W.; Krishnamoorti, R.; Reichart, G. C.; Balsara, N. P.; Fetters, L. J.; Lohse, D. J. *Macromolecules* **1995**, *28*, 1260.
(6) Maranas, J. K.; Kumar, S. K.; Debenedetti, P. G.; Graessley, W. W.; Mondello, M.; Grest, G. S. *Macromolecules* **1998**, *31*, 6998.
(7) Weimann, P. A.; Jones, T. D.; Hillmyer, M. A.; Bates, F. S.; Londono, J. D.; Melnichenko, Y.; Wignall, G. D.; Almdal, K. *Macromolecules* **1997**, *30*, 3650.
(8) White, J. L.; Lohse, D. J. *Macromolecules* **1999**, *32*, 958.
(9) Yamaguchi, M.; Miyata, H. *Macromolecules* **1999**, *32*, 5911.
(10) Wolak, J. E.; Jia, X.; White, J. L. *J. Am. Chem. Soc.* **2003**, *125*, 13660.
(11) Wolak, J.; Jia, X.; Gracz, H.; Stejskal, E. O.; White, J. L.; Wachowicz, M.; Jurga, S. *Macromolecules* **2003**, *36*, 4844.
(12) Maranas, J. K.; Mondello, M.; Grest, G. S.; Kumar, S. K.; Debenedetti, P. G.; Graessley, W. W. *Macromolecules* **1998**, *31*, 6991.
(13) Wolak, J. E.; White, J. L. *Macromolecules* **2005**, *38*, 10466.
(14) Krygier, E.; Lin, G. X.; Mendes, J.; Mukandela, G.; Azar, D.; Jones, A. A.; Pathak, J. A.; Colby, R. H.; Kumar, S. K.; Floudas, G.; Krishnamoorti, R.; Faust, R. *Macromolecules* **2005**, *38*, 7721.
(15) Cangialosi, D.; Alegria, A.; Colmenero, J. *Macromolecules* **2006**, *39*, 7149.
(16) Cangialosi, D.; Alegria, A.; Colmenero, J. *Macromolecules* **2006**, *39*, 448.
(17) Schwartz, G. A.; Cangialosi, D.; Alegria, A.; Colmenero, J. *J. Chem. Phys.* **2006**, *124*, 154904.

(18) deAzevedo, E. R.; Hu, W. G.; Bonagamba, T. J.; Schmidt-Rohr, K. *J. Am. Chem. Soc.* **1999**, *121*, 8411.
(19) deAzevedo, E. R.; Hu, W. G.; Bonagamba, T. J.; Schmidt-Rohr, K. *J. Chem. Phys.* **2000**, *112*, 8988.
(20) Miyoshi, T.; Pascui, O.; Reichert, D. *Macromolecules* **2004**, *37*, 6460.
(21) deAzevedo, E. R.; Tozoni, J. R.; Schmidt-Rohr, K.; Bonagamba, T. J. *J. Chem. Phys.* **2005**, *122*, 154506.
(22) Lemenestrel, C.; Kenwright, A. M.; Sergot, P.; Laupretre, F.; Monnerie, L. *Macromolecules* **1992**, *25*, 3020.
(23) Chung, G. C.; Kornfield, J. A.; Smith, S. D. *Macromolecules* **1994**, *27*, 964.
(24) Walton, J. H.; Miller, J. B.; Roland, C. M.; Nagode, J. B. *Macromolecules* **1993**, *26*, 4052.
(25) Wachowicz, M.; Wolak, J.; Gracz, H.; Stejskal, E. O.; Jurga, S.; McCord, E. F.; White, J. L. *Macromolecules* **2004**, *37*, 4573.
(26) Wefing, S.; Kaufmann, S.; Spiess, H. W. *J. Chem. Phys.* **1988**, *89*, 1234.
(27) O'Connor, R. D.; Ginsburg, E. J.; Blum, F. D. *J. Chem. Phys.* **2000**, *112*, 7247.
(28) Luz, Z.; Tekely, P.; Reichert, D. *Prog. Nucl. Magn. Reson. Spectrosc.* **2002**, *41*, 83.
(29) Wolak, J. E.; Knutson, J.; Martin, J. D.; Boyle, P.; Sargent, A. L.; White, J. L. *J. Phys. Chem. B* **2003**, *107*, 13293.
(30) Kaufmann, S.; Wefing, S.; Schaefer, D.; Spiess, H. W. *J. Chem. Phys.* **1990**, *93*, 197.
(31) Fox, T. G. *Am. Phys. Soc.* **1965**, *1*, 123.
(32) Wolynes, P. G. *J. Res. Natl. Inst. Stand. Technol.* **1997**, *102*, 187.
(33) Richert, R.; Angell, C. A. *J. Chem. Phys.* **1998**, *108*, 9016.
(34) Bisquert, J.; Henn, F.; Giuntini, J. C. *J. Chem. Phys.* **2005**, *122*, 094507.
(35) Sastry, S. *Nature (London)* **2001**, *409*, 164.
(36) Tracht, U.; Wilhelm, M.; Heuer, A.; Feng, H.; Schmidt-Rohr, K.; Spiess, H. W. *Phys. Rev. Lett.* **1998**, *81*, 2727.
(37) Brekner, M. J.; Schneider, H. A.; Cantow, H. J. *Polymer* **1988**, *29*, 78.
(38) Adam, G.; Gibbs, J. H. *J. Chem. Phys.* **1965**, *43*, 139.

MA070605G